Detrending crop yield data for spatial visualization of drought impacts in the United States, 1895-2014

Junyu Lu [*], Gregory J. Carbone, Peng Gao

Department of Geography, University of South Carolina, Columbia, South Carolina 29208, United States

Abstract: Historical drought events have had severe impacts on United States agriculture, but attempts to quantify and compare these impacts across space and time have been challenging because of the nonlinear and non-stationary nature of the crop yield time series. Here, we address this challenge using long-term state- and county-level corn yield data from 1895 to 2014. We apply and compare six trend simulation models – simple linear regression, second order polynomial regression, centered moving average, locally weighted regression, spline smoothing, and empirical mode decomposition – to simulate the nonlinear trend, and two decomposition models – an additive decomposition model and a multiplicative decomposition model – to remove the nonlinear trend from the yield time series. Our comparison of each method evaluates their respective advantages and disadvantages with respect to applicability across time and space, efficiency, and robustness. We find that a locally weighted regression model, coupled with a multiplicative decomposition model, is the most appropriate data self-adaptive detrending method. Detrended crop yield minus one represents the percentage lower or higher than normal yield conditions, termed “crop yield anomaly”. We then apply this detrending method and perform correlation analysis to show the quantitative relationship between state-level corn yield

[*] Corresponding author: Department of Geography, University of South Carolina, 709 Bull Street, Columbia, South Carolina 29208, United States.
E-mail address: jlu@email.sc.edu

anomalies and multiple drought indices. We find that the 3-month Standardized Precipitation Index (SPI) in August and Palmer Z-index in July correlate most closely with corn yield anomalies. This correlation is higher east of the 100˚ W meridian, where irrigation is not as extensively used. Finally, we show how the detrending process allows spatial visualization of drought impact on corn yield in the US using gridded August 3-month SPI values with examples from six major droughts on corn yields. Our focus on comparing detrending methods produces a methodology that can aid analysis of agricultural yield for both empirical and modeling studies connecting environmental and climate conditions to crop productivity.

Keywords: Detrending method; Crop yield anomaly; Locally weighted regression model; Drought index; Gridded Standardized Precipitation Index

1. Introduction

Drought is a devastating, recurring, and widespread natural hazard that affects natural habitats, ecosystems, and economic and social sectors, such as agriculture, transportation, industry, and urban water supply (Heim, 2002). The magnitude of drought impacts depends on various factors, including timing, duration, and severity, as well as a region's vulnerability, sensitivity, and adaptive capacity (Wheaton et al., 2008), which makes quantification of overall drought impacts difficult. Within the agricultural sector, droughts reduce soil-water availability, affect water and soil quality, increase risks of wildfire and pest infestation, and contribute to crop failures and pasture losses. Droughts can severely affect crop growth and reduce yield, threatening our food security. Despite tremendous improvements in technology and in crop yield potential, food production and food security remain highly dependent on weather and climate variation (Rosenzweig et al., 2001).

Droughts have had large economic impacts on US agriculture. From 1980 to 2014 alone, CPI (Consumer Price Index) - adjusted drought losses are estimated at $206B (NOAA, 2016). The 1930s Dust Bowl (three major waves: 1934, 1936, and 1939-1940), with its sustained deficient rainfall, high temperatures, and high winds, reduced the yield of wheat and corn by as much as 50% (NOAA, 2003; Warrick, 1984). The 1950s drought reached its greatest spatial extent in 1954, when crop yields in some areas dropped as much as 50% (NOAA, 2003). The 1987-1989 drought caused estimated total losses of $39B in energy, water, ecosystems, and agriculture (Riebsame et al., 1991) and resulted in about a 30% reduction in US corn production (Rosenzweig et al., 2001). About 80 percent of agricultural land experienced drought in 2012, making the 2012 drought the most extensive since the 1950s (USDA, 2013). The 2012 drought resulted in widespread harvest failures of the corn, sorghum, and soybean and caused agriculture damage up to be $30B (NOAA, 2016). Such studies have chronicled total agricultural losses during individual event. However, few studies have compared these losses across events because of challenges associated with changing technology and other non-climatic influences on yield.

The impact of an extreme weather event on agriculture depends not only on the severity of the event itself, but also on the time of the event and the vulnerability of the natural systems that experience it (IPCC, 2012; Lesk et al., 2016; van der Velde et al., 2012). Similar extreme weather could have differing outcomes depending on the crop development stages and the vulnerability of the exposed system (e.g., irrigation and technology would mitigate such vulnerability to drought) (Lesk et al., 2016; van der Velde et al., 2012). Thus, identifying the spatiotemporal variation of the drought impacts on agriculture and constructing a quantitative relationship between drought and agriculture losses could provide policy makers and stakeholders with scientific information regarding which agricultural areas are most vulnerable and sensitive to drought.

Quantifying and comparing drought losses across time and space are challenging because crop yields and productions are controlled by many factors, including scientific and technological advances (e.g., improvements in plant genetics, fertilizer, pesticides, and irrigation facilities), as well as weather and climate factors. The overall trend is of increasing yield, mainly caused by technological advances; the high-frequency fluctuations are mainly caused by weather and climate factors (Appendix A, Fig. A1). All of these factors make long-term crop yield data inherently nonlinear and non-stationary (varying mean and standard deviation). This renders comparison and spatial visualization of drought impact on agriculture difficult. For example, the 1950s droughts (peaking in 1954) and the 2012 drought are two historical major events. It is difficult to quantitatively extract and compare the impacts of these two droughts on agriculture merely from the original crop yield maps because of yield differences caused by technological advances and spatial patterns of agricultural production (Appendix A, Fig. A2). Modeling and spatial visualization of drought impacts on agriculture require appropriate distinctions between the high frequency fluctuations caused by the climate variability and the long-term trend caused by technological factors. This study explores and introduces a process of identifying the long-term trend, appropriately detrending yield data, and separating out a meaningful climate effect on crop yield.

Detrending technology statistically removes the long-term mean changes from the time series. The trend should be removed before other basic applications are implemented, such as computing the correlation function (Wu et al., 2007). Most previous studies detrended crop yield using a specific predetermined function, such as a simple linear regression model or a second order polynomial regression model against time. For example, Quiring and Papakryiakou (2003) applied a simple linear regression model to detrend wheat yield data; the resulting residuals were used to determine the most appropriate drought indices for measuring agricultural drought in the Canadian prairies. Trnka et al. (2007) applied a second order polynomial regression model to detrend yield data to evaluate the effect of drought on the spring barley crop. Goldblum (2009) applied a simple linear regression model to detrend soybean yield and a quadratic regression model to detrend corn yield. Residuals from a regression line served as estimates of detrended crop yield to examine the impacts of climate variability. Hlavinka et al. (2009) applied second order polynomials to capture long-term crop yield trend and used residuals to describe yield response to drought in the Czech Republic. Mishra and Cherkauer (2010) used a best-fit least squares linear regression method to detrend crop yield, identifying drought impacts during three crop growth periods in Illinois and Indiana.

However, the simple linear regression model and second order polynomial regression model used in previous studies are not suitable to detrend long-term crop yield in this study. Such predetermined functions cannot accommodate nonlinearity seen in the crop yield time series, as illustrated by data from five select states (Appendix A, Fig. A1). Additionally, the detrending process must be done across space, involving yield data for dozens of states and thousands of counties. Predetermined functions also lack sufficient flexibility and capability to remove many different nonlinear trends from the data, because trends vary across space (Appendix A, Fig. A1). Furthermore, potential future climate changes in mean and variability, combined with technological changes, could introduce additional nonlinearity and non-stationarity to crop yield data in the long-term. Thus, a data self-adaptive detrending method that can automatically follow the underlying pattern of the nonlinear crop yield time series is needed.

This study compares six trend simulation methods and two decomposition models, and evaluates their respective advantages and disadvantages with respect to applicability across time and space, efficiency, and robustness. We explore an appropriate data self-adaptive detrending approach that can automatically simulate the long-term nonlinear and non-stationary yield trend caused mainly by technology advances and thus remove the trend to isolate interannual fluctuations caused mainly by weather and climate factors. By applying this approach to detrend and standardize the corn yield data, we construct a quantitative relationship between drought and agriculture losses and compare drought impacts on corn yield across time and space through spatial visualization from 1895 to 2014 by highlighting six major historical drought events.

2. Data source and methodology

2.1 Agriculture data

Long-term agriculture statistics were obtained from USDA's National Agricultural Statistics Service (NASS), which maintains a comprehensive database of land use, farm income, crop production and yield, livestock, and commodity prices at national, regional, state, and county levels (USDA, 2014). Since the mid-1950's, NASS estimates have been derived from area frame surveys which identify cultivated areas from remotely-sensed imagery, followed by stratified sampling in random field locations. This method is complemented by farmer interviews within regions of highest cultivation. NASS collects information from several sources, of which the sample surveys are the most important. Further detail on sampling methods and uncertainty analysis is available elsewhere (Davies, 2009; Prince et al., 2001; USDA, 1983; USDA, 1999; USDA, 2006; USDA, 2012; USDA, 2016). We examined corn yield because corn is the most widely produced crop in the US. We compared detrending methods and demonstrated spatial visualizations of drought impacts on corn yield from 1895 to 2014 for 48 states and 2398 out of 3108 counties with at least 30-year corn yield data across the conterminous United States.

2.2 In-situ drought indices

State-level drought indices—including the monthly Palmer Drought Severity Index (PDSI), Palmer Hydrological Drought Index (PHDI), Palmer Z-index, Modified Palmer Drought Severity Index (PMDI), 1-month SPI (Standardized Precipitation Index), 2-month SPI, 3-month SPI, 6-month SPI, 9-month SPI, 12-month SPI, and 24-month SPI— from 1895 to 2015 were obtained from NOAA's National Centers for Environmental Information (ftp://ftp.ncdc.noaa.gov/). NCEI employs a climatologically-aided interpolation method to interpolate station data to composite grids; climate divisional and state values were computed as the area-weighted average of the composite gridpoints (Vose et al., 2014).

PDSI was developed by Palmer (1965), which is based on the supply-and-demand concept of the water balance equation by using precipitation, temperature and available water content (AWC) of the soil. It has three variations for different applications: Palmer Z index (Palmer, 1965) is used to measure short-term departure of moisture from normal; PHDI (Palmer, 1965) is used for water supply monitoring; and PMDI (Heddinghaus and Sabol, 1991) is designed for real-time operational purposes. The categories of drought intensity for PDSI, PHDI and PMDI are: 0 to -0.49 (near normal), -0.50 to -0.99 (incipient drought), -1.00 to -1.99 (mild drought), -2.00 to -2.99 (moderate drought), -3.00 to -3.99 (severe drought), and $\leqslant$ -4.00 (extreme drought). The categories of drought intensity for Palmer Z index are: 0 to -1.24 (near normal), -1.25 to -1.99 (mild to moderate drought), -2.00 to -2.74 (severe drought), and $\leqslant$ -2.75 (extreme drought). SPI was developed by McKee et al. (1993) to quantify precipitation deficit for different time scales.

More information about drought indices can be found in the reviews of Heim (2002), Mishra and Singh (2010), and WMO and GWP (2016).

We calculated 4-km gridded SPI values across the conterminous United States using 4-km PRISM (Parameter-elevation Relationships on Independent Slopes Model) precipitation dataset (Daly et al., 2008) from 1895 to 2014 for the spatial visualization purpose in section 3.4. SPI values were computed following the method of McKee et al. (1993). For each pixel, monthly precipitations can be accumulated into different time scales (e.g. 1-month, 2-month, 3-month, 6-month, 9-month, 12-month, and 24-month). For zero precipitation accumulation, the probability was computed using the frequency of zero precipitation accumulation. For non-zero precipitation accumulation, a two-parameter gamma distribution was fitted by using the maximum likelihood estimation (MLE) method. Then, the probability of zero and non-zero precipitation accumulation together was transformed into the quantile of a normal distribution with mean of zero and standard deviation of one by using inverse normal (Gaussian) distribution function. The resulting value is SPI. The different time scales for SPI are computed to address various types of drought: the shorter time scales are appropriate for meteorological drought and agricultural drought, the longer time scales are for hydrological drought (Heim, 2002; McKee et al., 1993). McKee et al. (1993) has defined drought intensities for values of the SPI into four categories: 0 to -0.99 (mild drought), -1.00 to -1.49 (moderate drought), -1.50 to -1.99 (severe drought), and $\leqslant$ -2.00 (extreme drought).

2.3 Detrending method

We compared six different detrending methods for removing the increasing trend from corn yield. The first step of detrending is to simulate the trend inherent in the data. The trend simulation methods included a simple linear regression model, a second order polynomial regression model, a moving average model, a locally weighted regression model (LOWESS), a smoothing spline model, and an empirical mode decomposition model (EMD). After trend simulation, we applied and compared two decomposition models to detrend the data. These methods were applied separately for each state and each county. All data processing and spatial visualization used the R programming language and its related packages.

2.3.1 Trend simulation method

2.3.1.1 Simple linear regression model

A simple linear regression model is the most commonly used statistical method to identify a linear trend. By visual inspection, if the trend is linear, a simple linear regression fitting would be sufficient to simulate the trend. The resulting trend is a straight line fitted to the data. Simple linear regression model can be fitted against time using the method of least squares. $Y_t = \beta_0 + \beta_1 t$

Where Y_t is the crop yield at time t; time t is the predictor; and β_0 and β_1 are the coefficients.

2.3.1.2 Second order polynomial regression model

A second order polynomial regression model is also commonly used in trend simulation (Goldblum, 2009; Hlavinka et al., 2009; Trnka et al., 2007). A second order polynomial regression model is appropriate if a quadratic trend present in the crop yield time series. This model accounts for the positive trend in annual crop yield that occurs because of increasing fertilization, plant genetics, and technological innovation and then declines because of economic transformation in the farming sector (Chloupek et al., 2004; Hlavinka et al., 2009). A second order polynomial regression model can be fitted against time using the method of least square.

$$Y_t = \beta_0 + \beta_1 t + \beta_2 t^2$$

Where Y_t is the crop yield at time t; time t is the predictor; and β_0, β_1, and β_2 are the coefficients.

2.3.1.3 Moving average model

Moving average models can be used to smooth the irregular roughness and high-frequency variation to identify overall pattern and trend in a time series. The moving average model is data self-adaptive. Unlike linear regression models, moving average models do not provide a specific model, but they detect local trends that simple linear regression models cannot. There are two simple kinds of moving average models: backward moving average (BMA) models, wherein all values for previous years are averaged for specific time spans, and centered moving average (CMA) models, wherein the values are averaged both before and after the current time. BMA models introduce an artificial time shift between the original data and the moving average (Bashan et al., 2008). CMA models are preferred because they eliminate this artificial effect. As the time span of moving average increases, the trend becomes smoother. Here, CMAs at time spans of 5 years, 10 years, 15 years, and 20 years are calculated to identify the trend. Formulas for each time span are as follows:

5 years: $mY_t = \frac{1}{5}Y_{t-2} + \frac{1}{5}Y_{t-1} + \frac{1}{5}Y_t + \frac{1}{5}Y_{t+1} + \frac{1}{5}Y_{t+2}$

10 years: $mY_t = \frac{1}{20}Y_{t-5} + \sum_{j=-4}^{4}\frac{1}{10}Y_{t+j} + \frac{1}{20}Y_{t+5}$

15 years: $mY_t = \sum_{j=-7}^{7}\frac{1}{15}Y_{t+j}$

20 years: $mY_t = \frac{1}{40}Y_{t-10} + \sum_{j=-9}^{9}\frac{1}{20}Y_{t+j} + \frac{1}{40}Y_{t+10}$

Where Y_t is the original crop yield at time t; and mY_t is the moving averaged crop yield at time t.

2.3.1.4 Locally weighted regression model

The locally weighted regression model (LOWESS) is a widely used non-parametric regression smoothing and memory-based method proposed by Cleveland (1979) and further developed by Cleveland and Devlin (1988). LOWESS involves a regression model based on a weighted least squares method that uses a local point of interest and assigns more weights to neighboring points near the point of interest and less weights to points farther away. The regression model can be linear or polynomial. Locally quadratic fitting performs better when the regression surface has substantial curvature (Cleveland and Devlin, 1988). LOWESS requires a weight function and fraction of points in the neighborhood (*f*) parameter (neighborhood size). Here, the weight function is a tri-cube weight function, and the weight for any specific point in the neighborhood is determined by the distance between that point and the point of interest.

Here, we use the locally weighted quadratic fitting. In this procedure, we let $0<f\leq 1$ and let r be fn rounded to the nearest integer (n is total data points). The integer r is the number of points used to estimate the point of interest t_i. Let d_{max} be the time difference between t_i and the rth nearest neighbor. For each t_i, the weight function W are defined for all t_k (k = 1, …, n) as follows

$$w_{t_k}(t_i) = \left(1 - \left|\frac{t_k - t_i}{d_{\max}}\right|^3\right)^3 \left(w_{t_k}(t_i) = 0,\ for\ |t_k - t_i| \geq d_{\max}\right)$$

For each t_i, the estimates $\hat{\beta}_0(t_i)$, $\hat{\beta}_1(t_i)$, and $\hat{\beta}_2(t_i)$ of $\beta_0(t_i)$, $\beta_1(t_i)$, and $\beta_2(t_i)$ are fitted by method of weighted least squares with weight function W to minimize

$$\sum_{k=1}^{n} w_{t_k}(t_i)(Y_{t_k} - \beta_0(t_i) - \beta_1(t_i)t_k - \beta_2(t_i)t_k^{\ 2})^2$$

Thus, the fitted value $\hat{Y}_{t_i}$ at time t_i using locally weighted quadratic fitting is

$$\hat{Y}_{t_i} = \hat{\beta}_0(t_i) + \hat{\beta}_1(t_i)t_i + \hat{\beta}_2(t_i)t_i^{\ 2}$$

As the fraction of points in the neighborhood (*f*) increases, more points will be included in the regression of the point of interest and the regression will become more global. More detailed information about LOWESS can be found in Cleveland (1979) and Cleveland and Devlin (1988). Setting the parameter *f* is a critical issue in LOWESS. Cross validation provides an appropriate method to determine the optimum parameter *f*. In this study, *f* was determined by the k-fold cross validation method, which is a data self-adaptive automatic method (Stone, 1974). The original sample data are randomly partitioned into k mutually disjoint equal-sized groups. Each time, one group is left out for validation and the remaining k-1 groups are used as training data for prediction. With k iterations, all sample data are used for both training and validation and each group is used once as validation data. The averaged prediction error (mean absolute error) of k times is used for cross-validation statistics. The parameter *f* with the minimum averaged prediction error is used as the optimum parameter. The R function “crossval” in the R package “bootstrap” was used for cross-validation implementation for LOWESS method (Efron and Tibshirani, 1993)

2.3.1.5 Smoothing spline model

Spline functions have been applied extensively for interpolation. A *k*th order spline is a piecewise continuous polynomial function of degree k and has continuous derivatives of order 1, 2, … and k-1, at its knot points. Splines are superior to polynomials for approximating disjointed or episodic functions, where ordinary polynomials are inadequate (Cook and Peters, 1981). Reinsch (1967) developed an algorithm for spline smoothing to extract the underlying function from unwanted experimental noise. Spline smoothing uses a penalized least squares criterion to control for overfitting by shrinking the effect of the standard sum-of-square functions for a regression spline and adding the roughness “penalty” regularization function (differentiable function) (Eubank, 1988).

Cubic smoothing spline model is the most commonly used method and will be used in this study. Let Y_{t_i} be crop yield at time t_i, modeled by function $Y_{t_i} = f(t_i)\ (i = 1,2,\ldots,n)$. The smoothing spline estimate $\hat{f}$ of the function *f* is defined to minimize

$$\sum_{i=1}^{n}(Y_{t_i} - f(t_i))^2 + \lambda\int_{t_1}^{t_n}(f''(t))^2 dt$$

The smoothing parameter λ is a tuning parameter governing the trade-off between the goodness of fit and smoothness of the curve. As λ approaches zero, the smoothing spline emphasizes goodness of fit and the curve converges to the traditional interpolation spline passing through each of the data points. As λ approaches positive infinity, the smoothing spline emphasizes smoothness and the curve converges to a straight line of ordinary linear regression (Eubank, 1988). The most important issue for spline smoothing is to find an objective criterion for choosing the optimum value of the smoothing parameter λ. Wahba and Craven (1978) proposed the generalized cross validation (GCV) method for spline smoothing; it is the method currently recognized as optimal for parameter selection.

2.3.1.6 Empirical mode decomposition model

Huang et al. (1998) have developed an empirical mode decomposition (EMD) method for analyzing nonlinear and non-stationary data. The method decomposes a complicated data set into different "intrinsic mode functions" (IMF) based on the local characteristic time scale of the data. The method is intuitive, direct, and adaptive (Huang et al., 1998). An intrinsic mode function satisfies two conditions: (1) in the whole data set, the number of extrema and the number of zero crossings must be either equal or differ at most by one; (2) at any point, the mean value of the envelope defined by the local maxima and the envelope defined by the local minima is zero (Huang et al., 1998). The IMFs represent the oscillation mode embedded in the data and are extracted systematically in a sifting process. The sifting process identifies the local maxima and minima to extract from the highest-frequency oscillation to lowest-frequency oscillation systematically until the residual component becomes a constant, a monotonic function where no more complete IMF can be identified, or the residue becomes so small that it is less than the predetermined value of substantial consequence (Huang et al., 1998; Wu et al., 2007). Finally, a data set will be decomposed approximately into $\log_2 n$ IMFs, with n being the number of data points (Wu et al., 2007) and the decompose equation is as follows:

$$Y(t) = \sum_{j=1}^{m} c_j + r_m$$

Where m is the total number of IMFs; c_j is the jth IMF; and r_m is the residual component. More detailed information about EMD method can be found in Huang et al. (1998), Huang et al. (2003) and Wu and Huang (2004).

2.3.2 Decomposition model

After simulating the trend by appropriate statistical models, a decomposition model is applied to remove the simulated trend and obtain the detrended data. There are two methods to do this:

The simplest method is an additive decomposition model. Generally, the composition of fluctuations and trend is assumed to be additive. The detrended data result from subtracting the values of the trend line from the original data, creating a time series of residuals. The unit of the residuals is the same as the original data. An additive decomposition model is appropriate when the variation is relatively constant over time.

Another method is a multiplicative decomposition model, wherein the detrended data result from computing the ratio of the original data to the values of the trend line. The detrended data are dimensionless and indicate percentage differences compared to the values of the trend line. A multiplicative decomposition model is appropriate when the variation is not constant through time. The multiplicative decomposition model can remove the variance associated with the trend.

2.4 Quantitative measures of trend fitting

Six basic quantitative measures of trend fitting were used in this study: root mean square error (RMSE), mean absolute error (MAE), coefficient of efficiency (E), index of agreement (d), modified coefficient of efficiency (E_1), and modified index of agreement (d_1).

Root mean square error (RMSE) and mean absolute error (MAE) have been widely used as standard statistical metrics to measure model performance. Nash and Sutcliffe (1970) defined the coefficient of efficiency (E) as the proportion of the initial variance accounted for by a model. It ranges from minus infinity to 1.0 with higher values indicating better agreement. Willmott (1981) proposed the index of agreement (d) to represent 1 minus the ratio between the sum of squared errors (SSE) and the "potential error" (PE). It ranges from 0.0 to 1.0 with higher values indicating better agreement between the model and observation. Both d and E represent an improvement over the widely used coefficient of determination (R^2). R^2 describes the degree of collinearity between the observed and simulated values, but this measure is limited by its insensitivity to additive and proportional differences between observations and model simulations (Legates and Davis, 1997; Legates and McCabe, 1999; Willmott, 1981). Both d and E can detect differences in the observed and model simulated means and variances.

Further, Willmott (1984) and Legates and McCabe (1999) argued that both d and E are sensitive to outliers because errors and differences are inflated when their values are squared. Based on original d and E, Willmott et al. (1985) and Legates and McCabe (1999) proposed a more generic form of d and E and advocated the use of the modified index of agreement (d_1) and the modified coefficient of efficiency (E_1). The advantage of d_1 and E_1 is that the errors and differences are given appropriate weighting, not inflated by their squared values (Legates and McCabe, 1999).

Table 1. Equation of quantitative measures of trend fitting

	Equation		Equation
Root Mean Square Error (RMSE)	$RMSE=\sqrt{\frac{1}{n}\sum_{i=1}^{n}(y_i-\hat{y}_i)^2}$	Mean Absolute Error (MAE)	$MAE=\frac{1}{n}\sum_{i=1}^{n}\lvert y_i-\hat{y}_i\rvert$
Coefficient of Efficiency (E)	$E=1-\frac{\sum_{i=1}^{n}(y_i-\hat{y}_i)^2}{\sum_{i=1}^{n}(y_i-\bar{y})^2}$	Modified Coefficient of Efficiency (E_1)	$E_1=1-\frac{\sum_{i=1}^{n}\lvert y_i-\hat{y}_i\rvert}{\sum_{i=1}^{n}\lvert y_i-\bar{y}\rvert}$
Index of Agreement (d)	$d=1-\frac{\sum_{i=1}^{n}(y_i-\hat{y}_i)^2}{\sum_{i=1}^{n}(\lvert\hat{y}_i-\bar{y}\rvert+\lvert y_i-\bar{y}\rvert)^2}$	Modified Index of Agreement (d_1)	$d_1=1-\frac{\sum_{i=1}^{n}\lvert y_i-\hat{y}_i\rvert}{\sum_{i=1}^{n}(\lvert\hat{y}_i-\bar{y}\rvert+\lvert y_i-\bar{y}\rvert)}$

Where y_i represents the *i*th observed value; $\hat{y}_i$ represents the *i*th model simulated value; $\bar{y}$ represents the observation mean for the entire period.

3. Results

3.1 Detrending methods comparison

3.1.1 Trend simulation methods comparison

Fig. 1 shows the corn yield time series from 1895 to 2014 in Illinois and South Carolina, as well as the trend simulation results by six models. Both the corn yield time series in Illinois and South Carolina show a prominent nonlinear increasing trend dominates the long-term crop yield time series. The trend is largely due to technological development and increasing inputs, and is most pronounced after 1950. The series also show high-frequency variation, largely due to weather-related factors, that increases with time. In order to isolate the interannual variability, it is necessary to remove the technology trend from the time series to standardize crop yield.

Because the technology trend is nonlinear, a simple linear regression model does not explain the change of corn yield in Illinois (Fig. 1-1(a)) and South Carolina (Fig. 1-2(a)) well and is not logical or reasonable for detrending long-term crop yield data. A quadratic trend improves the relationship in Illinois (Fig. 1-1(b)), but it still cannot capture the slowly increasing trend from

1895 to1960 in South Carolina (Fig. 1-2(b)). A second order polynomial regression model fit the trend well for several states (e.g., Idaho, Illinois, Maryland, Michigan, and Minnesota), but not in many others. These pre-selected models lack sufficient flexibility to remove the non-stationary and nonlinear trend for all states and all counties.

Visual inspection of corn yield suggests that a 20-year CMA model is necessary to smooth the irregularities in the time series (Fig. 1-1(c) and Fig. 1-2(c)). A moving average model requires a predetermined time span to do the moving average operation. However, the determination and the choice of time span for a moving average model is subjective. In addition, a boundary problem arises when using the CMA model. A 20-year CMA model requires 10-years of data before and after the year of interest. As the data point moves to the earliest or latest years, the first 10 and last 10 data points, respectively, lack enough data to be estimated and are assigned as missing values (Fig. 1-1(c) and Fig. 1-2(c)). Furthermore, one missing value occurring in the time series can cause 20 additional data points to be assigned as missing values for the moving average trend curve. But, even if no missing values exist in the time series, a 20-year CMA still sacrifice 20 data points at the earliest and latest data points of the time series. The centered moving average model is of no use or biased near the boundary of the time series.

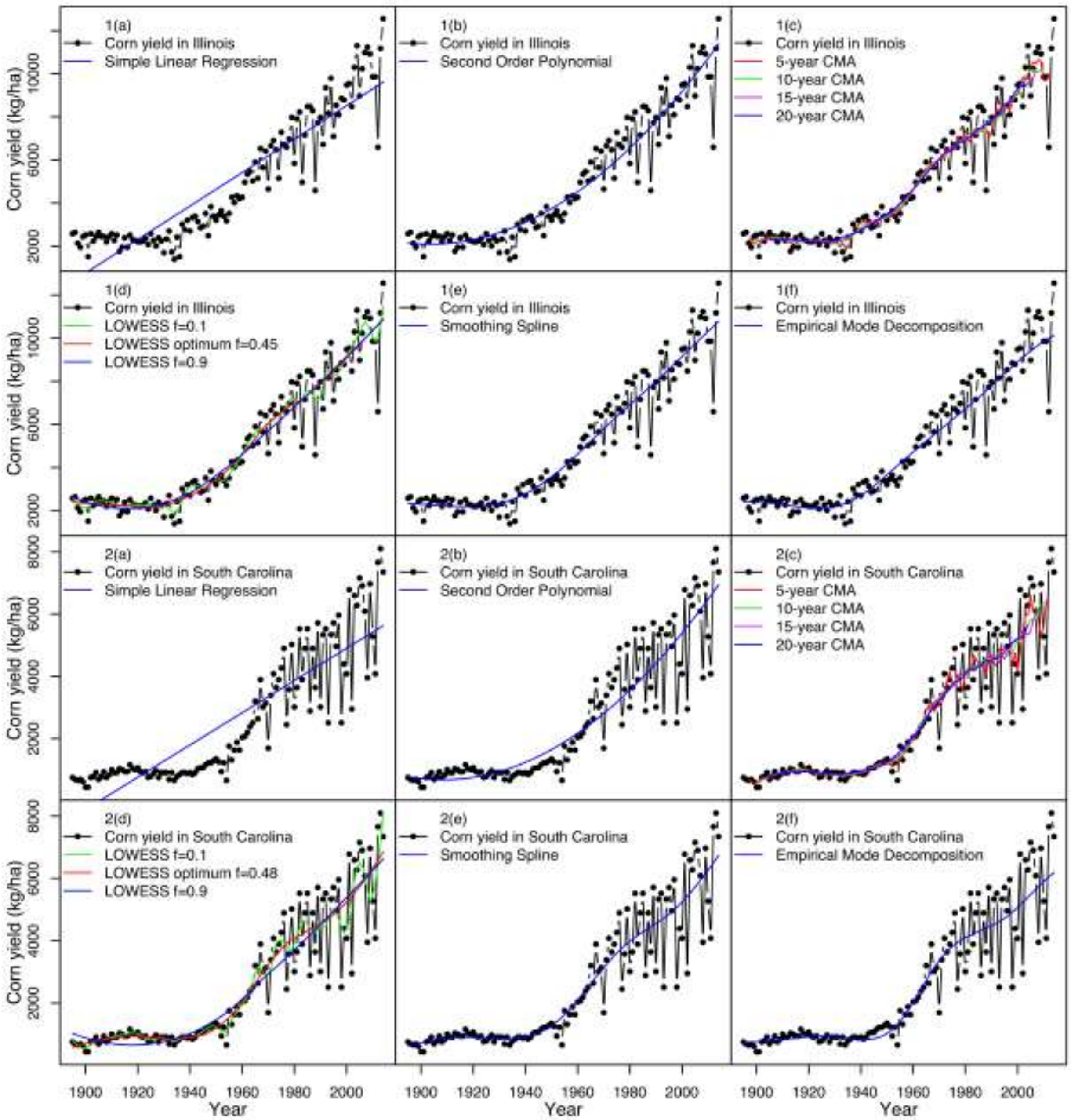

Fig. 1. Trend simulation methods comparison: (a) simple linear regression model; (b) second order polynomial model; (c) centered moving average model of 5-year, 10-year, 15-year, and 20-year timespans; (d) locally weighted regression model; (e) smoothing spline model; (f) empirical mode decomposition model (the upper six figures are Illinois and the lower six figures are South Carolina; data: corn yield from 1895 to 2014 in Illinois and South Carolina)

By contrast, LOWESS models can be fitted with neighboring points near the boundary of the time series and the boundary points can be estimated instead of being assigned as missing values. LOWESS models can be either linear or polynomial. Locally weighted quadratic fitting performs better when the regression surface has substantial curvature (Cleveland and Devlin, 1988), like that of corn yield through time. Here, we use locally weighted quadratic fitting in this study. In the LOWESS method, choice of the parameter f (fraction of points in the neighborhood) is very critical. As f increases from 0.1 to 1, the scale of the trend changes from local to global (Fig. 1-1(d) and Fig. 1-2(d)). With an f parameter of 1, LOWESS includes all of the data in the time series, and it is actually a polynomial regression model performed on the whole time series (Cleveland and Devlin, 1988). Here, we used a ten-fold cross-validation process to optimize the choice of f (Breiman and Spector, 1992). The ten-fold cross-validation process was repeated 100 times and the average parameter f was used as the optimum value for each state and county. One assumption of the LOWESS methodology is that the fitted function should follow the underlying patterns of the data providing a nearly unbiased estimation (Cleveland and Devlin, 1988). Visual inspection for trending fitting of state-level corn yield demonstrates that the fitted trend using the optimum f parameter corresponds to the underlying time series pattern, such as Illinois (Fig. 1-1(d)) and South Carolina (Fig. 1-2(d)).

For the smoothing spline model, we used generalized cross validation (GCV) to optimize the smoothing parameter. The trend curve simulated by the smoothing spline model also follows the corn yield time series closely in Illinois (Fig. 1-1(e)) and South Carolina (Fig. 1-2(e)), and this model performs well for most corn yields at the state level. However, for counties with shorter records, the fitted smoothing spline passes through all data points and converges to a traditional interpolation spline that no longer smooths the data, losing its ability to fit the long-term trend caused by technological advances (examples of four counties are shown in Fig. 2).

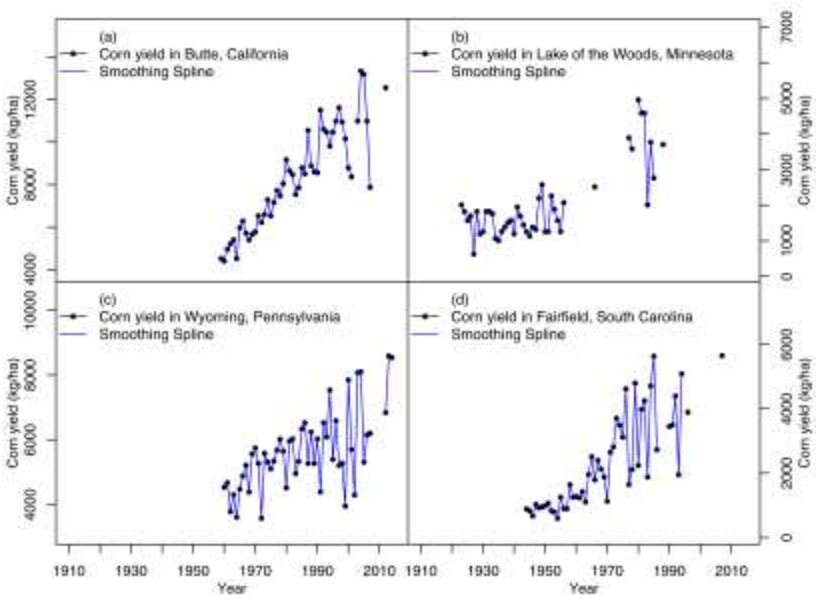

Fig. 2. Smoothing spline trend simulations for (a) Butte, California; (b) Lake of the Woods, Minnesota; (c) Wyoming, Pennsylvania; (d) Fairfield, South Carolina (smoothing spline converges to traditional interpolation spline)

For the empirical mode decomposition (EMD) model, the residual component is a monotonic function or a function containing only a single extrema from which no more oscillatory IMFs can be extracted (Huang et al., 1998). The residual component can represent the overall trend, which is determined intrinsically and is neither linear nor quadratic (Wu et al., 2007). The definition of the residual component in EMD method is almost identical to the definition of the trend when the data span in the trend covers the whole data length (Wu et al., 2007). Visual inspection suggests that the residual component of an EMD model simulated the trend well following the intrinsic data pattern through time in 35 out of 48 states, such as Illinois (Fig. 1-1(f)) and South Carolina (Fig. 1-2(f)). In another 11 states, the trend should include the residual component and the lowest-frequency IMF that contains physically meaningful information. In the remaining two states, the trend should include the residual component and the two lowest-frequency IMFs to represent the trend.

3.1.2 Quantitative measure of trend fitting results

Table 2. Quantitative measures of trend fitting results

	RMSE	MAE	E	d	E_1	d_1
Simple Linear Regression Model	1219.19	1041.38	80%	94%	57%	77%
Second Order Polynomial Regression Model	743.37	545.49	92%	98%	77%	88%
20-year Centered Moving Average Model	554.31	375.42	93%	98%	81%	90%
Locally Weighted Regression Model	559.56	374.85	95%	99%	84%	92%
Spline Smoothing Model	531.85	357.10	95%	99%	84%	92%
Empirical Mode Decomposition Model	592.36	403.80	94%	98%	82%	91%

Notes: the units of RMSE and MAE are the same with corn yield: kg/ha; the units of E, d, E_1, and d_1 are percent.

Table 2 shows the average values of the 48 states for six quantitative measures of trend fitting to provide an overall perspective of trend fitting for those six trend simulation methods. For state-level data, in all six measures, simple linear regression models are the poorest fitting model, while second order polynomial regression models provide a closer fit to the observed data when compared with simple linear regression models. The other four methods all perform much better than simple linear regression models and second order polynomial regression models, fitting state-level corn yield with similar accuracy.

The modified index of agreement (d_1) ranges from 0 to 1.0, while modified coefficient of efficiency (E_1) ranges from minus infinity to 1.0. The modified index of agreement (d_1) is more convenient for interpretation (Legates and McCabe, 1999), and thus we calculated the county-level d_1 to compare the county-level trend fitting for different methods (Fig. 3). EMD model is not included in the county-level analysis, because the choices of residual components and the IMFs of EMD model to fit the trend are not consistent for different counties and EMD model needs visual inspection and manual applications, which is not practical for thousands of counties. Further, the counties where the smoothing spline converges to an interpolation spline will be excluded from calculation of d_1 because an interpolation spline connects all data points and renders a useless fit for the technological trend (Fig. 3). The county-level d_1 for the other four methods are shown in (Fig. 3(a-d)); those for the smoothing spline are shown in (Fig. 3(e)) where about 600 counties are excluded because of this convergence. Fig. 3 shows that the d_1 of locally weighted regression models are higher than with the simple linear regression models, second order polynomial models, and 20-year centered moving average models. The d_1 of locally weighted regression and smoothing spline are close. Given the limitation of smoothing spline model on shorter records, locally weighted regression models represent the best trend fit for county-level corn yield data in terms of modified index of agreement (d_1).

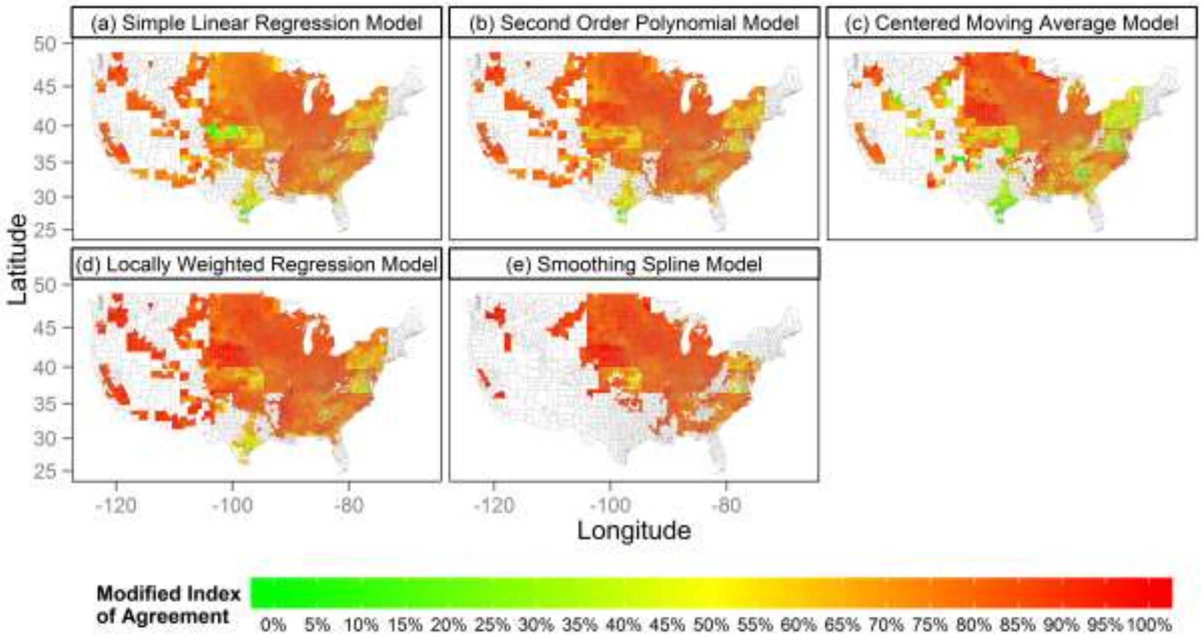

Fig. 3. County-level modified index of agreement (d_1) in the United States for five trend simulation methods: (a) simple linear regression model; (b) second order polynomial regression model; (c) 20-year centered moving average model; (d) locally weighted regression model; (e) smoothing spline model

3.1.3 Decomposition models comparison

The studies conducted by Hlavinka et al. (2009), Quiring and Papakryiakou (2003), Trnka et al. (2007), Goldblum (2009) and Mishra and Cherkauer (2010) assumed an additive composition of fluctuations and trends, and used residuals subtracted from the regression line as the detrended data to represent crop departure from normal. However, we found evidence to suggest that this may not be a sound assumption for long-term corn yield time series in this study.

After applying an additive decomposition model to remove the trend from the time series, the variance of detrended corn yield in both Illinois and South Carolina increases with time (Fig. 4). As corn yield and associated variance increase with time, the variance of the differences between original crop yield and simulated trend also increases. Thus, a multiplicative decomposition model is more appropriate because the variance of the detrended data is adjusted to the magnitude of crop yield, becoming more stationary through time (Fig. 4). Here, detrended crop yields minus one represent the percentage lower or higher than normal crop yield conditions (i.e. extreme events don't occur); these values are denoted as "crop yield anomalies". Therefore, after implementing an appropriate trend simulation method, we applied a multiplicative decomposition model to detrend corn yield.

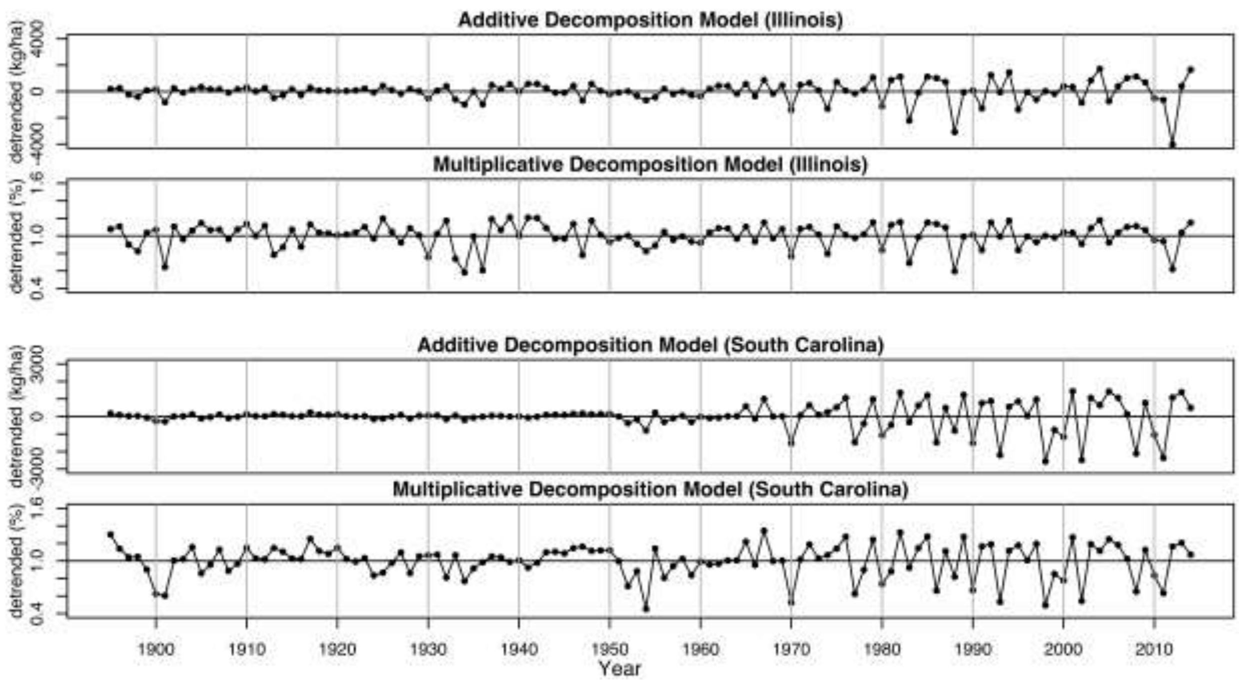

Fig. 4. Comparison of additive decomposition model and multiplicative decomposition model (the upper two figures are Illinois and the lower two figures are South Carolina; data: corn yield from 1895 to 2014 in Illinois and South Carolina; trend simulation method: locally weighted regression model)

3.2 Final detrending model choice

Our choice of a detrending model is based on performance, efficiency, and robustness. The analysis above demonstrates the sub-par performance of the simple linear regression and second order polynomial regression models. Further, the centered moving average model is of no use and/or is biased near the boundaries of the time series, as well as being strongly limited by missing values. The empirical mode decomposition model performs well for state-level corn yield data, but, as discussed in section 3.1.1, the choice of the residual component and the IMFs is not consistent across the United States, requiring visual inspections and manual applications. Employing EMD to detrend multiple crop types in thousands of counties is time consuming and not practical. The smoothing spline model performs well for state-level corn yield where the records are long, but it does not perform well for shorter records. For counties with shorter data records (e.g., fewer than 60 years), the smoothing spline converges to interpolation spline and connects all data points together, rendering it useless for this application (Fig. 2). The spline smoothing model is not robust to data with shorter records for fitting the trend caused by technological advances. The locally weighted regression model can automatically follow the underlying pattern of the non-linear and nonstationary corn yield time series and provide good trending fitting for both state-level and county-level corn yield. Thus, the locally weighted regression model coupled with multiplicative decomposition model is the preferred method here to detrend the corn yield for both state-level and county-level, and is then employed in the following analysis.

3.3 Correlation analysis between detrended crop yield and multiple drought indices

Corn has five main phenological stages: emerged, silking, dough, dent, and mature (USDA, 2009), and yield sensitivity to drought varies with stages. Corn is most sensitive to water stress during the early reproductive stage (tasseling, silking, and pollination) (Kranz et al., 2008). Droughts occur during silking period tend to desiccate the silks and pollen grains, causing poor pollination and resulting in the greatest yield reduction (Berglund et al., 2010; Kranz et al., 2008). We performed correlation analysis to examine the best drought indices to correlate with corn yield anomalies for spatial visualization purpose in section 3.4 and to demonstrate the spatial patterns of the correlations.

3-month SPI in August and Z-index in July show the highest correlation with corn yield anomalies among all of the drought indices (Fig. 5). Since the 3-month SPI in August is calculated from June, July, and August precipitation totals, it corresponds most closely to tasseling, silking, blister, milk, dough and dent stages. The phenology of corn explains why corn yield anomalies correlate most closely with 3-month SPI in August. As the time scale of SPI increases from 3-month to 24-month, the correlation coefficient decreases (Fig. 5). This indicates that time scale of 3-month for SPI is appropriate for agricultural drought monitoring.

For shorter time scales drought indices (1-month SPI, 2-month SPI, and Z-index), the corn yield anomalies are most highly correlated with drought indices in July (Fig. 5), suggesting that July is the most critical single month when averaged across the United States, because July approximately corresponds to the early reproductive stage (tasseling/silking) in most states. In some southern states (e.g., Texas), where corn planting and harvesting time are earlier (USDA, 2010), corn yield anomalies are most highly correlated with 1-month SPI, 2-month SPI and Z-index in June.

PDSI, PHDI, and PMDI show the highest correlation with corn yield anomalies in August among all seasons and perform better than the SPI at 6-month and longer time scales, but are inferior to the SPI at 3-month and shorter time scales as well as to the Z-index (Fig. 5).

The two maps showing the highest correlations (Z-index in July and 3-month SPI in August), indicate that the corn yield anomalies are more highly correlated with drought intensity east of 100˚ W meridian than west of it (Fig. 5). This occurs because areas west of the 100˚ W meridian typically use irrigation (Schlenker and Roberts, 2009). Those areas east of 100˚ W meridian usually do not, leaving them more susceptible to drought.

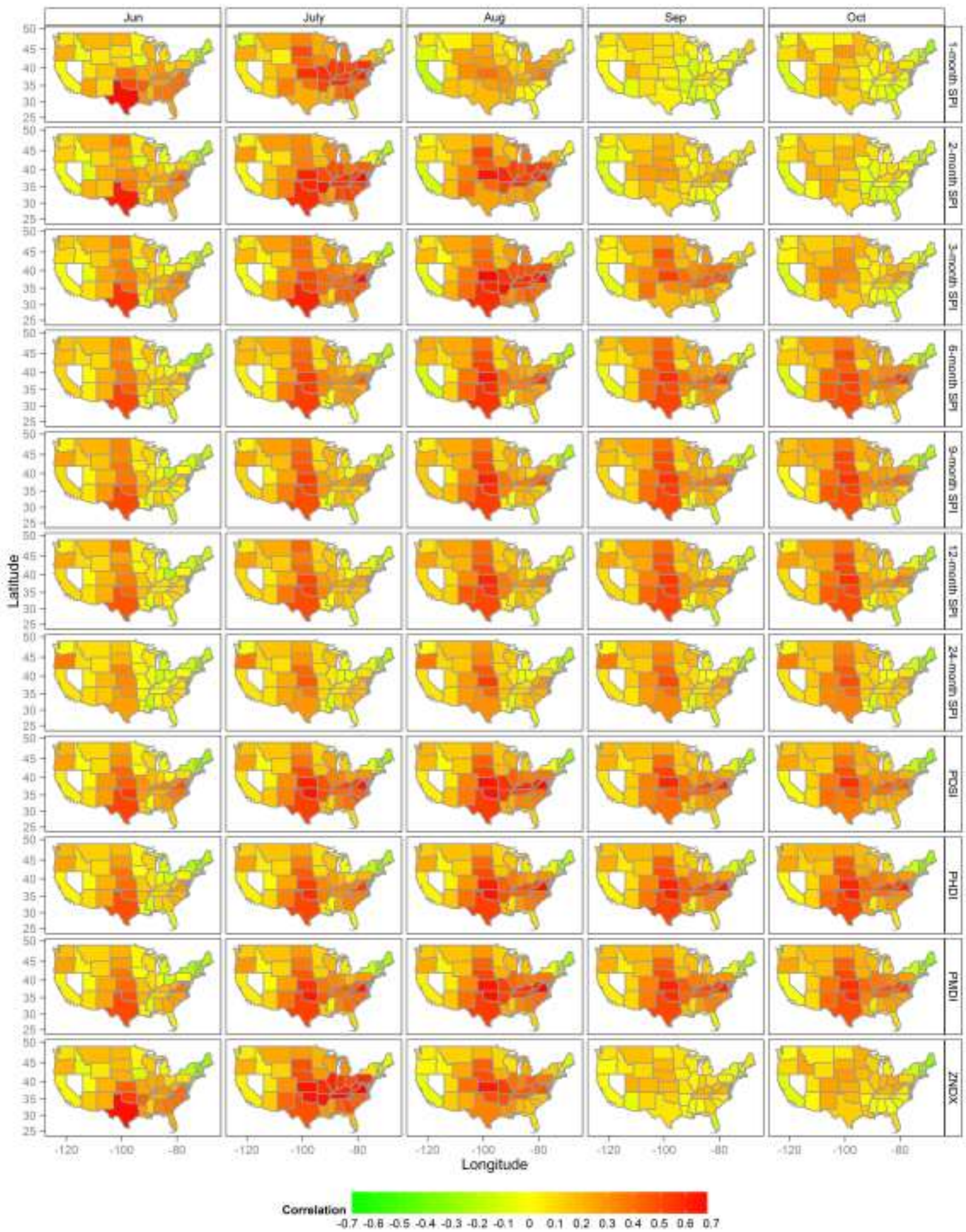

Fig. 5. Correlation maps of multiple drought indices by month with corn yield anomalies at state level (For example, the map in the second row and second column shows correlations between the 2-month SPI in July and corn yield anomalies at state level)

3.4 Spatial visualization of drought impact on crop yield

We used this detrending approach to compare corn yield responses to drought across six major drought years: the droughts of 1936, 1954, 1980, 1988, 2002, and 2012. We used only counties in the conterminous United States with at least 30 years of data (counties in white are either counties do not produce corn, or counties with missing data for a particular drought, or counties with too short records). The corn yield time series for each state and each county was detrended separately using a locally weighted regression model coupled with a multiplicative decomposition model. The values shown in maps (Fig. 6) are corn yield anomalies. Since the 3-month SPI in August and the Z-index in July show the highest correlation with corn yield anomalies, we used the gridded 3-month SPI in August calculated from the 4-km gridded PRISM data as a reference of drought severity.

The maps of state-level corn yield anomalies generally correspond well with the county-level maps (Fig. 6). The county-level maps clearly show more detailed crop information than the state-level maps (Fig. 6). The state-level and county-level maps complement each other to reflect crop yield anomalies information.

The crop yield anomalies were calculated by adjusting to the magnitude of the crop yield itself, which indicates percentage lower or higher than the crop yield of normal conditions. This methodology lets us compare drought impacts across space and time. The 1936 drought had the greatest impact on corn yield in the Midwest and parts of West South Central, where corn yields fell by 50% and more (Fig. 6). The impact of the 1954 drought showed up mainly in West South

Central, East South Central, and South Atlantic, where the corn yield was reduced by 40% to 50% (Fig. 6). The 1980 drought was similar in both magnitude and spatial extent to the 1954 drought. The 1988 drought's impact on corn yield was most evident in the Midwest, East South Central, and South Atlantic, where the corn yield reduced by 30% to 40% (Fig. 6). The 2002 drought had its greatest impact in the Middle Atlantic and South Atlantic, where the corn yields of Maryland, New Jersey, Ohio, Pennsylvania, Delaware, South Carolina, and Virginia were reduced by 30% to 40% (Fig. 6). The impact of the recent 2012 drought was most strongly seen in the corn yield in the Midwest and East South Central, where the corn yields were 30% lower than normal in Illinois, Indiana, and Tennessee, and were 40% to 50% lower in Kentucky and Missouri (Fig. 6). Comparisons between August 3-month SPI and corn yield anomalies for these six severe droughts show a strong correspondence between dryness and lower-than-normal corn yield for areas east of 100˚ W, however, this correspondence is weak for areas west of 100˚ W because of agricultural irrigation (Fig. 6). The areas where corn yield greatly reduced during these six droughts correspond to the areas that experienced severe drought without access to irrigation.

The magnitudes of corn yield reductions in 1936, 1954 and 1988 correspond to the impacts reported in the literature cited in the introduction part (NOAA, 2003; Rosenzweig et al., 2001; Warrick, 1984). This result partially illustrates the effectiveness and robustness of the selected detrending method.

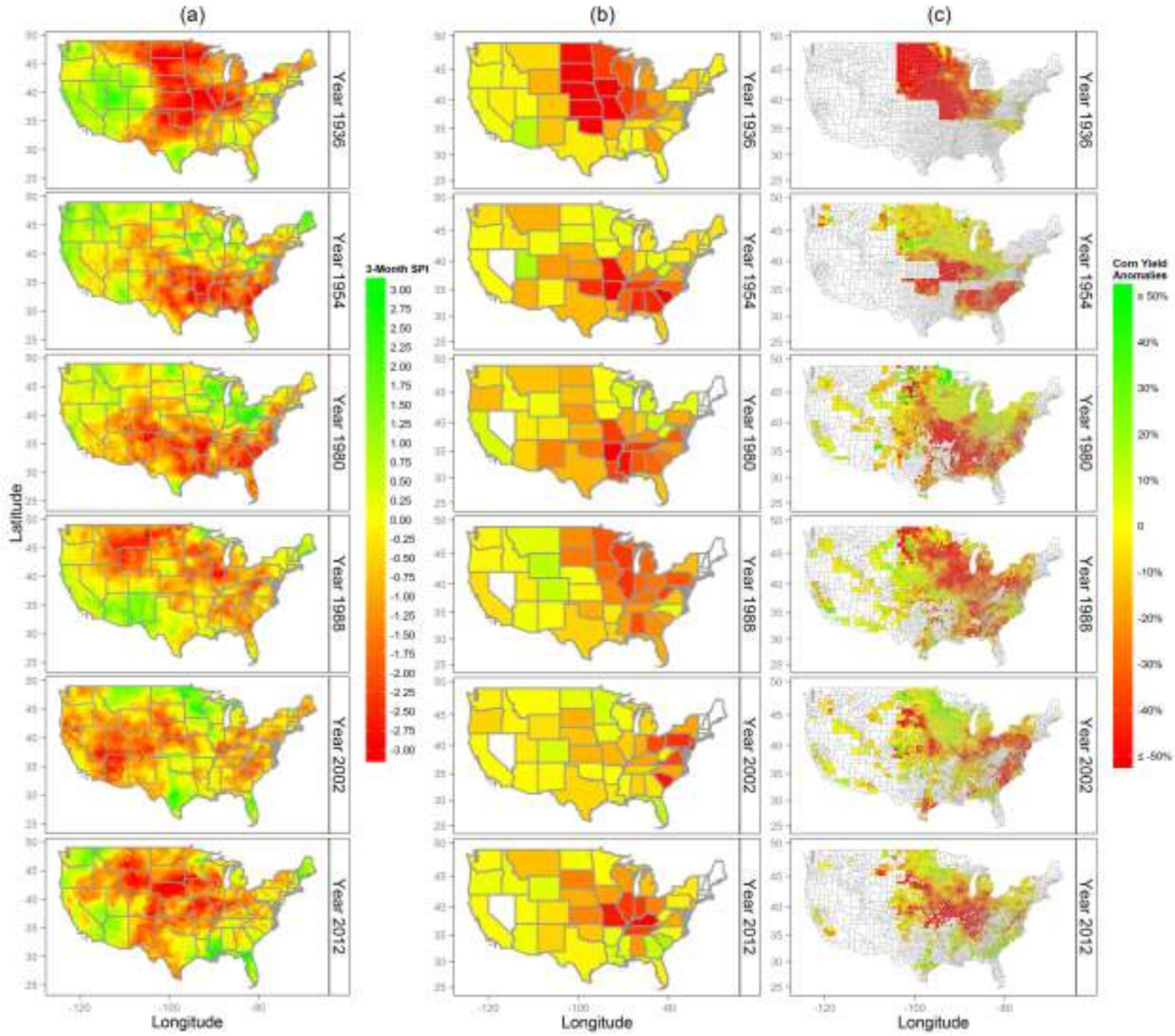

Fig. 6. Spatial visualization of state-level and county-level corn yield anomalies accompanied with gridded August 3-month SPI in the United States for six historical drought years: 1936, 1954, 1980, 1988, 2002, and 2012 (column (a): gridded August 3-month SPI calculated from PRISM data; column (b): state-level corn yield anomalies; column (c): county-level corn yield anomalies)

4. Discussion and conclusions

This study identifies the appropriate data self-adaptive detrending method to standardize and detrend the corn yield by comparing multiple detrending methods, in order to compare drought impacts on corn across both space and time. We compared six trend simulation methods using six quantitative measures of trend fitting and found that the simple linear regression and second order polynomial regression models have the poorest fit. Of the other four methods, the centered moving average model is limited by its boundary problems. Employing the EMD model to detrend crops for thousands of counties is time consuming and impractical because the choices of the residual component and IMFs to represent the trend are not consistent for different counties and different states and require visual inspections and manual applications. Smoothing spline models do not perform well for counties with shorter data records (e.g., fewer than 60 years) and in this case, a smoothing spline model connects all data points and converges to a traditional interpolation spline, which is useless in trend fitting for this application. We also compared two decomposition models and found that multiplicative decomposition model to be more appropriate for detrending crop yield because the variance of the detrended crop yield is adjusted according to the magnitude of crop yield and becomes more stationary over time. Thus, the locally weighted regression model, coupled with multiplicative decomposition model, is the most appropriate data self-adaptive method to detrend the crop yield.

This study represents the first long-term spatial visualization of drought impact on corn across large regions and identifies spatial patterns of the vulnerability of corn to drought in United States. Our approach standardized the corn yield allowing a quantitative measure of relationship between drought and corn yield and spatial visualization of drought impacts on corn yield. We performed correlation analysis between corn yield anomalies and multiple drought indices during growing seasons. Z-index in July and 3-month SPI in August are the best two drought indices to correlate with corn yield anomalies among all of the drought indices. The corn yield anomalies are more highly correlated with drought indices for states east of the 100˚ W meridian than the west of it. Six major drought years (1936, 1954, 1980, 1988, 2002, and 2012) were selected for the spatial visualization of drought impact on corn yield. Gridded 3-month SPI calculated from PRISM data were used to represent drought severity. The state-level and county-level maps of corn yield anomalies can capture the spatial variability of lower-than-normal corn yield caused by droughts. Lower-than-normal corn yield corresponds strongly with dryness east of 100˚ W, but weakly to its west. The impacts of the six historical droughts on corn yield were described and compared, and generally corresponded with what were reported in literature. This also illustrates the effectiveness and robustness of the selected detrending method.

Our detrending approach is not limited to corn and drought studies, but relevant to other crops and other natural hazards as well. We applied the same approach for soybeans. Strong correspondence was shown between dryness and lower-than-normal soybean yield in 1980 (Appendix A, Fig. A3). The 1980 drought showed its impact on soybean yield mainly in West South Central, East South Central, and South Atlantic and Kansas (Appendix A, Fig. A3). This approach is also not limited to drought analysis. Crop yield anomalies can occur for reasons other than drought (e.g., flooding, extreme short-term weather events, pest infestation, and disease). This study successfully separated out environmental and weather factors from other technological factors. By identifying crop yield anomalies, our approach can also be used, for example, to assess the effect of excessive moisture and flooding on crop yield. The Great Flood of 1993, occurring from April to September along the Mississippi and Missouri rivers and their tributaries, killed at least 48 people and caused approximately $20B in flood-related damages (Johnson et al., 2004). Corn yields in Midwest along the Mississippi and Missouri rivers were lower than normal (Fig. 7), mainly because of the flooding. The August 3-month SPI showed that, in contrast with the excessively wet conditions in Midwest, the Southeast experienced a severe drought (Fig. 7). The corn yields in the Southeast were also lower than the normal (Fig. 7), mainly due to the drought and heat wave.

Fig. 7. Spatial visualization of state-level and county-level corn yield anomalies accompanied with gridded August 3-month SPI in 1993: (a) gridded August 3-month SPI in 1993 calculated from PRISM data; (b) state-level corn yield anomalies in 1993; (c) county-level corn yield anomalies in 1993

Our approach provides one way to assess the impact of drought on crop yield, which could be useful in helping policy makers and stakeholders develop effective risk adaptation strategies and management plans to alleviate the impact of extreme weather on the agricultural sector. Furthermore, others have demonstrated the potential for crop production and yield prediction combining climate variables from GCMs and indices of observed antecedent sea surface temperature, warm water volume, and zonal wind patterns (Koide et al., 2013). Other example of locally weighted regression models have demonstrated skills for short-term forecasting (Lall et al., 2006). The method applied in this paper could also be used for short-term forecasts on the effect of technological changes on crop yield. As GCMs begin to demonstrate some success in decadal prediction (Meehl et al., 2014; van Oldenborgh et al., 2012), our method could be combined with such forecasts for predicting crop yield. Finally, the crop yield anomalies derived by this approach can also be used in the analysis of climate change impacts on agriculture.

Acknowledgements:

This work was supported by the National Oceanic and Atmospheric Administration (NOAA) Climate Program Office (grant number NA060AR4310007) to the Carolinas Integrated Sciences and Assessments. Here, we also wish to thank Karen Beidel for editorial assistance and suggestions.

Appendix A. Supplementary figures

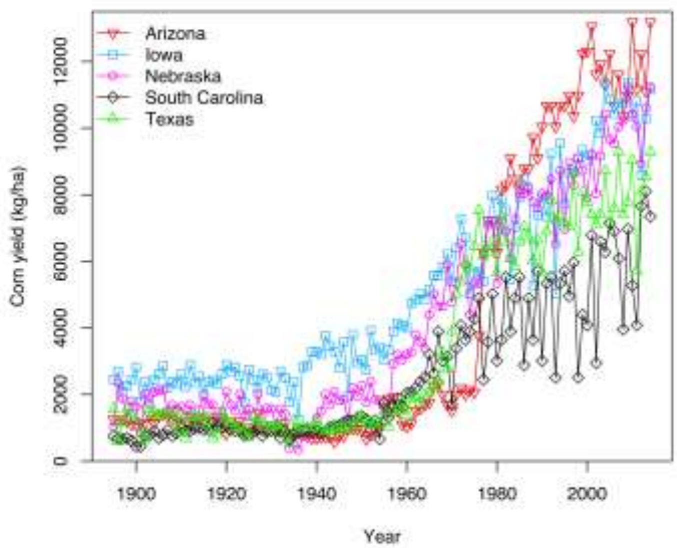

Fig. A1. Corn yield time series from 1895 to 2014 in Arizona, Iowa, Nebraska, South Carolina, and Texas (Units: kg/ha) (Corn yield data were obtained from USDA's National Agricultural Statistics Service; corn yields are calculated from corn production for grain divided by corn area harvested for grain.)

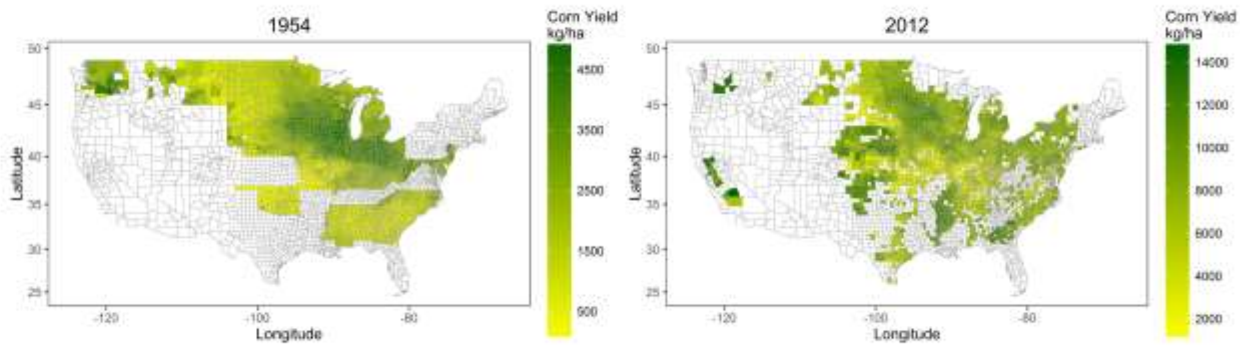

Fig. A2. Spatial visualization and comparison of original corn yield in 1954 and 2012 (Units: kg/ha)

Fig. A3. Spatial visualization of state-level and county-level soybean yield anomalies accompanied with gridded August 3-month SPI in 1980: (a) gridded August 3-month SPI in 1980 calculated from PRISM data; (b) state-level soybean yield anomalies in 1980; (c) county-level soybean yield anomalies in 1980

Reference:

Bashan, A., Bartsch, R., Kantelhardt, J.W. and Havlin, S., 2008. Comparison of detrending methods for fluctuation analysis. Physica A: Statistical Mechanics and its Applications, 387(21): 5080-5090.

Berglund, D.R., Endres, G.J. and McWilliams, D.A., 2010. Corn growth and management quick guide, North Dakota State University, Extension service, Fargo, North Dakota.

Breiman, L. and Spector, P., 1992. Submodel selection and evaluation in regression - the X-random case. Int Stat Rev, 60(3): 291-319.

Chloupek, O., Hrstkova, P. and Schweigert, P., 2004. Yield and its stability, crop diversity, adaptability and response to climate change, weather and fertilisation over 75 years in the Czech Republic in comparison to some European countries. Field Crops Research, 85(2–3): 167-190.

Cleveland, W.S., 1979. Robust Locally Weighted Regression and Smoothing Scatterplots. J. Am. Stat. Assoc., 74(368): 829-836.

Cleveland, W.S. and Devlin, S.J., 1988. Locally weighted regression: an approach to regression analysis by local fitting. J. Am. Stat. Assoc., 83(403): 596-610.

Cook, E.R. and Peters, K., 1981. The smoothing spline: a new approach to standardizing forest interior tree-ring width series for dendroclimatic studies. Tree-ring bulletin, 1981(41): 45-53.

Daly, C. et al., 2008. Physiographically sensitive mapping of climatological temperature and precipitation across the conterminous United States. Int. J. Climatol., 28(15): 2031-2064.

Davies, C., 2009. Area frame design for agricultural surveys, Research and Development Division, National Agricultural Statistics Service, U.S. Department of Agriculture, Washington DC.

Efron, B. and Tibshirani, R.J., 1993. An introduction to the bootstrap. Chapman & Hall/CRC, Boca Raton, London, New York, Washington, D.C.

Eubank, R.L., 1988. Spline smoothing and nonparametric regression. Marcel Dekker Inc, New York.

Goldblum, D., 2009. Sensitivity of corn and soybean yield in Illinois to air temperature and precipitation: the potential impact of future climate change. Phys. Geogr., 30(1): 27-42.

Heddinghaus, T.R. and Sabol, P., 1991. A review of the Palmer Drought Severity Index and where do we go from here, Proceedings of the seventh conference on applied climatology. American Meteorological Society Bos-ton, MA.

Heim, R.R., 2002. A review of twentieth-century drought indices used in the United States. B Am Meteorol Soc, 83(8): 1149-1165.

Hlavinka, P. et al., 2009. Effect of drought on yield variability of key crops in Czech Republic. Agr Forest Meteorol, 149(3-4): 431-442.

Huang, N.E. et al., 1998. The empirical mode decomposition and the Hilbert spectrum for nonlinear and non-stationary time series analysis. Proceedings: Mathematical, Physical and Engineering Sciences, 454(1971): 903-995.

Huang, N.E. et al., 2003. Applications of Hilbert-Huang transform to non-stationary financial time series analysis. Applied stochastic models in business and industry, 19(3): 245-268.

IPCC, 2012. Managing the risks of extreme events and disasters to advance climate change adaptation. A special report of working groups I and II of the Intergovernmental Panel on Climate Change (IPCC) [Field, C. B., V. Barros, T. F. Stocker, D. Qin, D. J. Dokken, K. L. Ebi, M. D. Mastrandrea, K. J. Mach, G.-K. PLattner, S. K. Allen, M. Tignor, and P. M. Midgley (eds.)]. Cambridge University Press, Cambridge, United Kingdom and New York, NY, USA, 582 pp.

Johnson, G.P., Holmes, R.R. and Waite, L.A., 2004. The great flood of 1993 on the upper mississippi river: 10 years later, US Department of the Interior, US Geological Survey.

Koide, N. et al., 2013. Prediction of rice production in the Philippines using seasonal climate forecasts. Journal of Applied Meteorology and Climatology, 52(3): 552-569.

Kranz, W.L., Irmak, S., Van Donk, S.J., Yonts, C.D. and Martin, D.L., 2008. Irrigation management for corn (NebGuide G1850), University of Nebraska, Lincoln, Lincoln, Nebraska.

Lall, U., Moon, Y.-I., Kwon, H.-H. and Bosworth, K., 2006. Locally weighted polynomial regression: Parameter choice and application to forecasts of the Great Salt Lake. Water Resour Res, 42(5): W05422.

Legates, D.R. and Davis, R.E., 1997. The continuing search for an anthropogenic climate change signal: Limitations of correlation-based approaches. Geophys. Res. Lett., 24(18): 2319-2322.

Legates, D.R. and McCabe, G.J., 1999. Evaluating the use of "goodness-of-fit" measures in hydrologic and hydroclimatic model validation. Water Resour Res, 35(1): 233-241.

Lesk, C., Rowhani, P. and Ramankutty, N., 2016. Influence of extreme weather disasters on global crop production. Nature, 529(7584): 84-87.

McKee, T.B., Doesken, N.J. and Kleist, J., 1993. The relationship of drought frequency and duration to time scales, Proceedings of the 8th Conference on Applied Climatology. American Meteorological Society Boston, MA, pp. 179-183.

Meehl, G.A. et al., 2014. Decadal climate prediction: An update from the trenches. B Am Meteorol Soc, 95(2): 243-267.

Mishra, A.K. and Singh, V.P., 2010. A review of drought concepts. J Hydrol, 391(1-2): 204-216.

Mishra, V. and Cherkauer, K.A., 2010. Retrospective droughts in the crop growing season: Implications to corn and soybean yield in the Midwestern United States. Agr Forest Meteorol, 150(7-8): 1030-1045.

Nash, J.E. and Sutcliffe, J.V., 1970. River flow forecasting through conceptual models part I — A discussion of principles. J Hydrol, 10(3): 282-290.

NOAA, 2003. North American drought: a paleo perspective. https://www.ncdc.noaa.gov/paleo/drought/drght_home.html (accessed 16.07.06).

NOAA, 2016. U.S. billion-dollar weather and climate disasters. https://www.ncdc.noaa.gov/billions/ (accessed 16.06.30).

Palmer, W.C., 1965. Meteorological drought, 30. US Department of Commerce, Weather Bureau Washington, DC, USA.

Prince, S.D., Haskett, J., Steininger, M., Strand, H. and Wright, R., 2001. Net primary production of U.S. Midwest croplands from agricultural harvest yield data. Ecological Applications, 11(4): 1194-1205.

Quiring, S.M. and Papakryiakou, T.N., 2003. An evaluation of agricultural drought indices for the Canadian prairies. Agr Forest Meteorol, 118(1-2): 49-62.

Reinsch, C., 1967. Smoothing by spline functions. Numer. Math., 10(3): 177-183.

Riebsame, W.E., Changnon Jr, S.A. and Karl, T.R., 1991. Drought and natural resources management in the United States. Impacts and implications of the 1987-89 drought. Westview Press Inc., Boulder, Colorado.

Rosenzweig, C., Iglesias, A., Yang, X.B., Epstein, P. and Chivian, E., 2001. Climate change and extreme weather events - implications for food production, plant diseases, and pests. Global Change & Human Health, 2(2): 90-104.

Schlenker, W. and Roberts, M.J., 2009. Nonlinear temperature effects indicate severe damages to US crop yields under climate change. P Natl Acad Sci USA, 106(37): 15594-15598.

Stone, M., 1974. Cross-Validatory choice and assessment of statistical predictions. J. R. Stat. Soc., 36(2): 111-147.

Trnka, M. et al., 2007. Agricultural drought and spring barley yields in the Czech Republic. Plant Soil Environ, 53(7): 306-316.

USDA, 1983. Scope and methods of the statistical reporting service, Statistical Reporting Service, U.S. Department of Agriculture, Washington, D.C.

USDA, 1999. Understanding USDA crop forecasts, National Agricultural Statistics Service, U.S. Department of Agriculture and Office of the Chief Economist, World Agricultural Outlook Board, Washington, D.C.

USDA, 2006. The yield forecasting program of NASS, the Statistical Methods Branch, Estimates Division, National Agricultural Statistics Service, U.S. Department of Agriculture, Washington, D.C.

USDA, 2009. National crop progress - terms and definitions. http://www.nass.usda.gov/Publications/National_Crop_Progress/Terms_and_Definitions/ (accessed 15.10.13).

USDA, 2010. Field crops usual planting and harvesting dates National Agricultural Statistics Service, U.S. Department of Agriculture, Washington, D.C.

USDA, 2012. The yield forecasting program of NASS, Statistical Methods Branch, Statistics Division, National Agricultural Statistics Service, U.S. Department of Agriculture, Washington, D.C.

USDA, 2013. U.S. drought 2012: farm and food impacts. http://www.ers.usda.gov/topics/in-the-news/us-drought-2012-farm-and-food-impacts.aspx (accessed 16.12.01).

USDA, 2014. United States Department of Agriculture - National Agricultural Statistics Service Database Quick Stats, Washington D.C.

USDA, 2016. History of agricultural statistics. https://www.nass.usda.gov/About_NASS/History_of_Ag_Statistics/ (accessed 16.12.01).

van der Velde, M., Tubiello, F.N., Vrieling, A. and Bouraoui, F., 2012. Impacts of extreme weather on wheat and maize in France: evaluating regional crop simulations against observed data. Clim. Chang., 113(3): 751-765.

van Oldenborgh, G.J., Doblas-Reyes, F.J., Wouters, B. and Hazeleger, W., 2012. Decadal prediction skill in a multi-model ensemble. Clim Dynam, 38(7): 1263-1280.

Vose, R.S. et al., 2014. Improved historical temperature and precipitation time series for U.S. climate divisions. Journal of Applied Meteorology and Climatology, 53(5): 1232-1251.

Wahba, G. and Craven, P., 1978. Smoothing noisy data with spline functions. estimating the correct degree of smoothing by the method of generalized cross-validation. Numer. Math., 31: 377-404.

Warrick, R., 1984. The possible impacts on wheat production of a recurrence of the 1930s drought in the U.S. Great Plains. Clim. Chang., 6(1): 5-26.

Wheaton, E., Kulshreshtha, S., Wittrock, V. and Koshida, G., 2008. Dry times: hard lessons from the Canadian drought of 2001 and 2002. The Canadian Geographer / Le Géographe canadien, 52(2): 241-262.

Willmott, C.J., 1981. On the validation of models. Phys. Geogr., 2(2): 184-194.

Willmott, C.J., 1984. On the evaluation of model performance in physical geography. In: G. Gaile and C. Willmott (Editors), Spatial Statistics and Models. Theory and Decision Library. Springer Netherlands, pp. 443-460.

Willmott, C.J. et al., 1985. Statistics for the evaluation and comparison of models. Journal of Geophysical Research: Oceans, 90(C5): 8995-9005.

WMO and GWP, 2016. Handbook of drought indicators and indices, Integrated Drought Management Programme (IDMP), Integrated Drought Management Tools and Guidelines Series 2, Geneva, Switzerland.

Wu, Z. and Huang, N.E., 2004. A study of the characteristics of white noise using the empirical mode decomposition method. Proc. R. Soc. Lond. A, 460(2046): 1597-1611.

Wu, Z., Huang, N.E., Long, S.R. and Peng, C.-K., 2007. On the trend, detrending, and variability of nonlinear and nonstationary time series. P Natl Acad Sci USA, 104(38): 14889-14894.